16th World Congress in Computational Mechanics (WCCM)
21-26 July 2024, Vancouver, Canada
A. Korobenko, M. Laforest, S. Prudhomme, R. Vaziri (Eds)

IMMERSED-BOUNDARY APPROACH BASED ON INTEGRATED RBFS AND SMOOTH EXTENSION FOR SOLVING PDES IN COMPLEX DOMAINS

N. Mai-Duy[1], **C.-D. Tran**[1], **D. Strunin**[2], **W. Karunasena**[1], **C.M.T. Tien**[3], **P. Yarlagadda**[1] **and Y.T. Gu**[4]

[1] School of Engineering
University of Southern Queensland, Toowoomba, QLD 4350, Australia
nam.mai-duy@unisq.edu.au, canh-dung.tran@unisq.edu.au, karu.karunasena@unisq.edu.au,
y.prasad@unisq.edu.au

[2] School of Mathematics, Physics and Computing
University of Southern Queensland, Toowoomba, QLD 4350, Australia
dmitry.strunin@unisq.edu.au

[3] Centre for Future Materials
University of Southern Queensland, Toowoomba, QLD 4350, Australia
camminhtri.tien@unisq.edu.au

[4] School of Mechanical, Medical and Process Engineering
Queensland University of Technology, Brisbane, QLD 4000, Australia
yuantong.gu@qut.edu.au

Key words: Immersed boundary, Smooth extension, Integrated radial basis functions, Five-point stencils.

Abstract. We propose an immersed-boundary approach, based on point collocation, five-point integrated radial basis function stencils, rectangular Cartesian grids and smooth extension of the solution, for solving the two-dimensional elliptic partial differential equation in a geometrically complex domain.

1 INTRODUCTION

When the partial differential equations (PDEs) are defined in rectangular domains, one can utilize high-order methods to solve them efficiently. For those methods, the domain is simply represented using Cartesian grids and high-order accuracy is achieved for case of smooth solution. For complex domains, the idea of embedding the physical domains into rectangular ones has received a great deal of attention. Examples of methods developed in this direction include the smooth selection embedding method [1] and the smooth forcing extension method [2]. They all require accurate imposition of the boundary conditions as well as smooth extension of the solution or the forcing function to a box in order to achieve high accuracy. In [1], to force the solution in the computational domain to be globally smooth, a high-order PDE outside the physical domain is solved, where all communication between the computational grid and the boundary is achieved by convolution with regularized delta-functions, and to acquire a highly accurate solution, Fourier spectral methods are employed. In [2], a Fourier extension method is applied to directly extend the forcing.

Radial basis functions (RBFs) have become an important tool in numerical analysis. In the integral (IRBF) approach, the RBFs are employed to represent a derivative and then integrated to obtain approximations for lower-order derivatives and a function itself. The integral approach enables the RBF approximations to avoid a reduction in the convergence rate caused by differentiation. In this work, the elliptic PDE is solved in a rectangular domain that covers the physical complex one. Like [1], a smooth extension of the solution to a box is carried out. Unlike [1], local approximations are employed to obtain a highly accurate discretization in the computational domain and the discretized system is modified to account for the presence of the immersed boundary [3, 4, 5, 6, 7]. The constants arising from the process of integrating the RBFs provide an effective means of including nodal derivative values of the field variable into the approximations. This inclusion can bring many benefits. For local stencils used in discretizing the PDE, it results in a significant improvement in the solution accuracy and enables the IRBF solution to be not influenced much by the RBF width. For the smooth extension problem, it enables the high-order PDE to be enforced at every interior grid node. The remainder of the paper is organized as follows. In Section 2, the proposed method is presented. In Section 3, numerical verification is carried out. Section 4 gives some concluding remarks.

2 PROPOSED METHOD

We describe the proposed method for its use in solving the Poisson equation

$$\frac{\partial^2 \bar{u}}{\partial x^2} + \frac{\partial^2 \bar{u}}{\partial y^2} = f \quad \text{in} \quad \Omega \tag{1}$$

where f is a forcing function and Ω is a physical multiply-connected domain (Figure 1). Let H be the hole regions. Cartesian grids are used to represent the computational domain, denoted by C, covering Ω and H (i.e., the square without holes). The approximations used in the proposed method are based on one-dimensional IRBFs. Let η represent the independent variables x and y, and v the dependent variables u^p (the solution in Ω) and u^h (the solution in H). In the η

direction, the variable v along a grid line is represented by using the following IRBF scheme

$$\frac{\partial^q v(\eta)}{\partial \eta^q} = \sum_{k=1}^{N_\eta} w_k G_k(\eta) = \sum_{k=1}^{N_\eta} w_k I_k^{(q)}(\eta), \tag{2}$$

$$\frac{\partial^{q-1} v(\eta)}{\partial \eta^{q-1}} = \sum_{k=1}^{N_\eta} w_k I_k^{(q-1)}(\eta) + c_1, \tag{3}$$

$$\cdots \quad \cdots \quad \cdots$$

$$\frac{\partial v(\eta)}{\partial \eta} = \sum_{k=1}^{N_\eta} w_k I_k^{(1)}(\eta) + c_1 \frac{\eta^{q-2}}{(q-2)!} + c_2 \frac{\eta^{q-3}}{(q-3)!} + \cdots + c_{q-1}, \tag{4}$$

$$v(\eta) = \sum_{k=1}^{N_\eta} w_k I_k^{(0)}(\eta) + c_1 \frac{\eta^{q-1}}{(q-1)!} + c_2 \frac{\eta^{q-2}}{(q-2)!} + \cdots + c_{q-1}\eta + c_q, \tag{5}$$

where N_η is the number of RBF centers (grid points) under consideration, $G_k(\eta)$ is the RBF, $I_k^{(q-1)}(\eta) = \int I_k^{(q)}(\eta) d\eta$, $I_k^{(q-2)}(\eta) = \int I_k^{(q-1)}(\eta) d\eta, \ldots, I_k^{(0)}(\eta) = \int I_k^{(1)}(\eta) d\eta$, $(w_1, w_2, \ldots, w_{N_\eta})$ the RBF coefficients, and $(c_1, c_2, \ldots, c_q)$ the integration constants. For the multiquadric function, $G_k(\eta) = \sqrt{(\eta - \eta_k)^2 + a_k^2}$, where η_k is the center and a_k is the width/shape-parameter. In (2)-(5), RBFs are integrated q times and we refer to it as an IRBF scheme of order q, denoted by IRBFq.

2.1 Discretizing the PDE without regard to the immersed boundary

Consider an interior node and its associated four neighbouring nodes (Figure 2). We apply the 1D IRBF scheme (2)-(5) to compute $\partial^2 u/\partial x^2$ and $\partial^2 u/\partial y^2$ at the central node (x_i, y_j). In the η direction, the IRBF approximation involves a set of 3 grid points $(\eta_{i-1}, \eta_i, \eta_{i+1})$ $(N_\eta = 3)$. For IRBFq, there are q integration constants and we utilise them to add q extra equations to the conversion of the RBF space into the physical space. It was shown in [5] that the IRBF solution is not influenced much by the RBF width when $q \geq 6$. In this work, $q = 6$ is implemented. In the following conversion system, the equations are employed to impose $(\partial^2 u/\partial \eta^2, \partial^3 u/\partial \eta^3, \partial^4 u/\partial \eta^4)$ at the two end-nodes

$$\widehat{u} = \mathcal{C}\widehat{w}, \tag{6}$$

where

$$\widehat{u} = \left(u_{i-1}, u_i, u_{i+1}, \frac{\partial^2 u_{i-1}}{\partial \eta^2}, \frac{\partial^2 u_{i+1}}{\partial \eta^2}, \frac{\partial^3 u_{i-1}}{\partial \eta^3}, \frac{\partial^3 u_{i+1}}{\partial \eta^3}, \frac{\partial^4 u_{i-1}}{\partial \eta^4}, \frac{\partial^4 u_{i+1}}{\partial \eta^4} \right)^T,$$

$$\widehat{w} = (w_1, w_2, w_3, c_1, c_2, c_3, c_4, c_5, c_6)^T,$$

and $\mathcal{C}$ is the matrix of size 9-by-9 (called the conversion matrix)

$$\mathcal{C} = \begin{bmatrix} I_1^{(0)}(\eta_{i-1}) & I_2^{(0)}(\eta_{i-1}) & I_3^{(0)}(\eta_{i-1}) & \frac{\eta_{i-1}^5}{5!} & \frac{\eta_{i-1}^4}{4!} & \frac{\eta_{i-1}^3}{3!} & \frac{\eta_{i-1}^2}{2} & \eta_{i-1} & 1 \\ I_1^{(0)}(\eta_i) & I_2^{(0)}(\eta_i) & I_3^{(0)}(\eta_i) & \frac{\eta_i^5}{5!} & \frac{\eta_i^4}{4!} & \frac{\eta_i^3}{3!} & \frac{\eta_i^2}{2} & \eta_i & 1 \\ I_1^{(0)}(\eta_{i+1}) & I_2^{(0)}(\eta_{i+1}) & I_3^{(0)}(\eta_{i+1}) & \frac{\eta_{i+1}^5}{5!} & \frac{\eta_{i+1}^4}{4!} & \frac{\eta_{i+1}^3}{3!} & \frac{\eta_{i+1}^2}{2} & \eta_{i+1} & 1 \\ I_1^{(2)}(\eta_{i-1}) & I_2^{(2)}(\eta_{i-1}) & I_3^{(2)}(\eta_{i-1}) & \frac{\eta_{i-1}^3}{3!} & \frac{\eta_{i-1}^2}{2} & \eta_{i-1} & 1 & 0 & 0 \\ I_1^{(2)}(\eta_{i+1}) & I_2^{(2)}(\eta_{i+1}) & I_3^{(2)}(\eta_{i+1}) & \frac{\eta_{i+1}^3}{3!} & \frac{\eta_{i+1}^2}{2} & \eta_{i+1} & 1 & 0 & 0 \\ I_1^{(3)}(\eta_{i-1}) & I_2^{(3)}(\eta_{i-1}) & I_3^{(3)}(\eta_{i-1}) & \frac{\eta_{i-1}^2}{2} & \eta_{i-1} & 1 & 0 & 0 & 0 \\ I_1^{(3)}(\eta_{i+1}) & I_2^{(3)}(\eta_{i+1}) & I_3^{(3)}(\eta_{i+1}) & \frac{\eta_{i+1}^2}{2} & \eta_{i-1} & 1 & 0 & 0 & 0 \\ I_1^{(4)}(\eta_{i-1}) & I_2^{(4)}(\eta_{i-1}) & I_3^{(4)}(\eta_{i-1}) & \eta_{i-1} & 1 & 0 & 0 & 0 & 0 \\ I_1^{(4)}(\eta_{i+1}) & I_2^{(4)}(\eta_{i+1}) & I_3^{(4)}(\eta_{i+1}) & \eta_{i+1} & 1 & 0 & 0 & 0 & 0 \end{bmatrix}.$$

Solving (6) yields

$$\widehat{w} = \mathcal{C}^{-1}\widehat{u}. \tag{7}$$

The second derivative of u at η_i is thus calculated by

$$\frac{\partial^2 u_i}{\partial \eta^2} = \mathcal{D}_{2\eta}\widehat{u}, \tag{8}$$

where $\mathcal{D}_{2\eta}$ is a row matrix of 9 coefficients that is defined as

$$\mathcal{D}_{2\eta} = \begin{bmatrix} I_1^{(2)}(\eta_i) & I_2^{(2)}(\eta_i) & I_3^{(2)}(\eta_i) & \frac{\eta_i^3}{3!} & \frac{\eta_i^2}{2} & \eta_i & 1 & 0 & 0 \end{bmatrix} \mathcal{C}^{-1}.$$

In practice, the coefficient set $\mathcal{D}_{2\eta}$ is acquired by using Gaussian elimination to solve the following algebraic equation set:

$$\mathcal{C}^T \mathcal{D}_{2\eta}^T = \left(I_1^{(2)}(\eta_i), I_2^{(2)}(\eta_i), I_3^{(2)}(\eta_i), \frac{\eta_i^3}{3!}, \frac{\eta_i^2}{2}, \eta_i, 1, 0, 0 \right)^T. \tag{9}$$

2.2 Modifying the discretized system to account for the presence of the immersed boundary

The stencils near the immersed boundary are modified to account for its presence. In each direction, we construct the approximation based on 4 nodes (three grid nodes: $(\eta_{i-1}, \eta_i, \eta_{i+1})$ and one boundary node: η_b) by also using IRBF6 (i.e. $q = 6$). Two configurations of nodes are shown in Figure 3; they share a common feature: there are two grid nodes in the physical domain and one grid node in the extension domain. The conversion system takes the form

$$\widehat{U} = \mathcal{C}_b \widehat{W}. \tag{10}$$

where

$$\widehat{U} = \left(u_{i-1}, u_i, u_{i+1}, u_b, \frac{\partial^2 u_{i-1}}{\partial \eta^2}, \frac{\partial^2 u_{i+1}}{\partial \eta^2}, \frac{\partial^3 u_{i-1}}{\partial \eta^3}, \frac{\partial^3 u_{i+1}}{\partial \eta^3}, \frac{\partial^4 u_{i-1}}{\partial \eta^4}, \frac{\partial^4 u_{i+1}}{\partial \eta^4} \right)^T,$$

$$\widehat{W} = (w_1, w_2, w_3, w_4, c_1, c_2, c_3, c_4, c_5, c_6)^T,$$

and $\mathcal{C}_b$ is the matrix of size 10-by-10

$$\mathcal{C} = \begin{bmatrix}
I_1^{(0)}(\eta_{i-1}) & I_2^{(0)}(\eta_{i-1}) & I_3^{(0)}(\eta_{i-1}) & I_4^{(0)}(\eta_{i-1}) & \frac{\eta_{i-1}^5}{5!} & \frac{\eta_{i-1}^4}{4!} & \frac{\eta_{i-1}^3}{3!} & \frac{\eta_{i-1}^2}{2} & \eta_{i-1} & 1 \\
I_1^{(0)}(\eta_i) & I_2^{(0)}(\eta_i) & I_3^{(0)}(\eta_i) & I_4^{(0)}(\eta_i) & \frac{\eta_i^5}{5!} & \frac{\eta_i^4}{4!} & \frac{\eta_i^3}{3!} & \frac{\eta_i^2}{2} & \eta_i & 1 \\
I_1^{(0)}(\eta_{i+1}) & I_2^{(0)}(\eta_{i+1}) & I_3^{(0)}(\eta_{i+1}) & I_4^{(0)}(\eta_{i+1}) & \frac{\eta_{i+1}^5}{5!} & \frac{\eta_{i+1}^4}{4!} & \frac{\eta_{i+1}^3}{3!} & \frac{\eta_{i+1}^2}{2} & \eta_{i+1} & 1 \\
I_1^{(0)}(\eta_b) & I_2^{(0)}(\eta_b) & I_3^{(0)}(\eta_b) & I_4^{(0)}(\eta_b) & \frac{\eta_b^5}{5!} & \frac{\eta_b^4}{4!} & \frac{\eta_b^3}{3!} & \frac{\eta_b^2}{2} & \eta_b & 1 \\
I_1^{(2)}(\eta_{i-1}) & I_2^{(2)}(\eta_{i-1}) & I_3^{(2)}(\eta_{i-1}) & I_4^{(2)}(\eta_{i-1}) & \frac{\eta_{i-1}^3}{3!} & \frac{\eta_{i-1}^2}{2} & \eta_{i-1} & 1 & 0 & 0 \\
I_1^{(2)}(\eta_{i+1}) & I_2^{(2)}(\eta_{i+1}) & I_3^{(2)}(\eta_{i+1}) & I_4^{(2)}(\eta_{i+1}) & \frac{\eta_{i+1}^3}{3!} & \frac{\eta_{i+1}^2}{2} & \eta_{i+1} & 1 & 0 & 0 \\
I_1^{(3)}(\eta_{i-1}) & I_2^{(3)}(\eta_{i-1}) & I_3^{(3)}(\eta_{i-1}) & I_4^{(3)}(\eta_{i-1}) & \frac{\eta_{i-1}^2}{2} & \eta_{i-1} & 1 & 0 & 0 & 0 \\
I_1^{(3)}(\eta_{i+1}) & I_2^{(3)}(\eta_{i+1}) & I_3^{(3)}(\eta_{i+1}) & I_4^{(3)}(\eta_{i+1}) & \frac{\eta_{i+1}^2}{2} & \eta_{i-1} & 1 & 0 & 0 & 0 \\
I_1^{(4)}(\eta_{i-1}) & I_2^{(4)}(\eta_{i-1}) & I_3^{(4)}(\eta_{i-1}) & I_4^{(4)}(\eta_{i-1}) & \eta_{i-1} & 1 & 0 & 0 & 0 & 0 \\
I_1^{(4)}(\eta_{i+1}) & I_2^{(4)}(\eta_{i+1}) & I_3^{(4)}(\eta_{i+1}) & I_4^{(4)}(\eta_{i+1}) & \eta_{i+1} & 1 & 0 & 0 & 0 & 0
\end{bmatrix}.$$

The only difference between $\widehat{U}$ in (10) and $\widehat{u}$ in (6) is that the former contains an extra value, u_b, which is the boundary condition on the immersed boundary. The second-order derivative of u at the central node of the stencil, i.e. $\partial^2 u_i/\partial\eta^2$, is now expressed in terms of u at $(\eta_{i-1}, \eta_i, \eta_{i+1}, \eta_b)$ and its nodal derivatives at only (η_{i-1}, η_{i+1}). When compared to (8), there is an additional term associated with u_b, which represents the effect of the immersed boundary on the discretization in the entire computational domain.

2.3 Constructing a smooth extension of the solution u into the computational domain C

To achieve high-order accuracy, the solution in a hole, u^h, should be constructed to be smooth across the hole's boundary. Assume that the solution in Ω, u^p, is a known function that is C^k continuous in Ω. In the smooth extension approach [1], the solution u^h is found by solving the following Kth-order PDE in a hole

$$\begin{cases} \mathcal{H}^K u^h = 0, \\ \frac{\partial^j u^h}{\partial n^j} = \frac{\partial^j u^p}{\partial n^j}, \end{cases} \tag{11}$$

where $\mathcal{H}^K$ is a high-order differential operator, $j = (0, 1, \ldots, k)$, $K = 2(k+1)$ and $\partial^j u/\partial n^j$ is the jth normal derivative of u on the hole's boundary. As discussed in [1], the system matrix becomes ill-conditioned for large k. In this work, the differential problem is solved iteratively. The solution at the previous iteration is known and we utilize it to derive the boundary conditions for the smooth extension problem (11). We also investigate the case of using $K < 2(k+1)$ and it will be shown that high-order accuracy is still achieved for $K = 4$ when $k \geq 2$. The lower the value of K the better the matrix condition number will be. After solving (11), we compute a forcing function associated with u^h.

For the global C^k regularity, the boundary values of u^h and its derivatives $(\partial u^h/\partial\eta, \ldots, \partial^k u^h/\partial\eta^k)$ are imposed. It is noted that $(\partial u^h/\partial x, \ldots, \partial^k u^h/\partial x^k)$ are for the horizontal grid lines, while

$(\partial u^h/\partial y, \ldots, \partial^k u^h/\partial y^k)$ are for the vertical grid lines. These boundary values are obtained after the IRBF approximations of u on the entire grid lines are carried out.

For each grid line in the extension domain, we employ IRBFq with $q = 2k$ to accommodate $2k$ boundary derivative values at the two end-nodes of the grid line. The conversion system takes the form

$$\widehat{u}_h = \mathcal{C}_h \widehat{w}_h. \tag{12}$$

where

$$\widehat{u}_h = \left(u_1^h, u_2^h, \ldots, u_{N_\eta}^h, \frac{\partial u_1^h}{\partial \eta}, \frac{\partial u_{N_\eta}^h}{\partial \eta}, \ldots, \frac{\partial^k u_1^h}{\partial \eta^k}, \frac{\partial^k u_{N_\eta}^h}{\partial \eta^k} \right)^T,$$

$$\widehat{w}_h = \left(w_1, w_2, \ldots, w_{N_\eta}, c_1, c_2, \ldots, c_{2k-1}, c_{2k} \right)^T,$$

and $\mathcal{C}_h$ is the matrix of size $(N_\eta + 2k)$-by-$(N_\eta + 2k)$

$$\mathcal{C}_h = \begin{bmatrix} I_1^{(0)}(\eta_1) & I_2^{(0)}(\eta_1) & \ldots & I_{N_\eta}^{(0)}(\eta_1) & \frac{\eta_1^{2k-1}}{(2k-1)!} & \ldots & \eta_1 & 1 \\ I_1^{(0)}(\eta_2) & I_2^{(0)}(\eta_2) & \ldots & I_{N_\eta}^{(0)}(\eta_2) & \frac{\eta_2^{2k-1}}{(2k-1)!} & \ldots & \eta_2 & 1 \\ \ldots & \ldots & \ldots & \ldots & \ldots & \ldots & \ldots & \ldots \\ I_1^{(0)}(\eta_{N_\eta}) & I_2^{(0)}(\eta_{N_\eta}) & \ldots & I_{N_\eta}^{(0)}(\eta_{N_\eta}) & \frac{\eta_{N_\eta}^{2k-1}}{(2k-1)!} & \ldots & \eta_{N_\eta} & 1 \\ I_1^{(1)}(\eta_1) & I_2^{(1)}(\eta_1) & \ldots & I_{N_\eta}^{(1)}(\eta_1) & \frac{\eta_1^{2k-2}}{(2k-2)!} & \ldots & 1 & 0 \\ I_1^{(1)}(\eta_{N_\eta}) & I_2^{(1)}(\eta_{N_\eta}) & \ldots & I_{N_\eta}^{(1)}(\eta_{N_\eta}) & \frac{\eta_{N_\eta}^{2k-2}}{(2k-2)!} & \ldots & 1 & 0 \\ \ldots & \ldots & \ldots & \ldots & \ldots & \ldots & \ldots & \ldots \\ I_1^{(k)}(\eta_1) & I_2^{(k)}(\eta_1) & \ldots & I_{N_\eta}^{(k)}(\eta_1) & \frac{\eta_1^{k-1}}{(k-1)!} & \ldots & 0 & 0 \\ I_1^{(k)}(\eta_{N_\eta}) & I_2^{(k)}(\eta_{N_\eta}) & \ldots & I_{N_\eta}^{(k)}(\eta_{N_\eta}) & \frac{\eta_{N_\eta}^{k-1}}{(k-1)!} & \ldots & 0 & 0 \end{bmatrix}.$$

Solving (12) yields

$$\widehat{w}_h = \mathcal{C}_h^{-1} \widehat{u}_h. \tag{13}$$

It is noted that value of N_η employed here is typically much smaller than the number of grid nodes of the entire grid line. Making use of (13), the derivatives of any order of the variable u^h with respect to x and y can be computed in terms of the nodal values of u^h and the boundary values of its derivatives. The advantage of incorporating the boundary conditions into the IRBF approximations is that it allows the equation in (11) to be enforced at every interior node.

2.3.1 Solving the resultant algebraic system

We apply the Newton method with finite-difference Jacobian to solve the resultant algebraic system. At each iteration, we carry out the following calculation tasks: (i) computes nodal values of derivatives of second order and higher ones along the grid lines using the 1D IRBF scheme [4], from which the boundary conditions (i.e. continuity conditions) for the Kth-order

PDE in the extension domain are acquired; (ii) solves the extension problem for u^h, from which the forcing function in the extension domain (i.e. F_h) is derived; (iii) modifies the forcing function by including new F_h; and (iv) updates the solution u in the computational domain. The approximation of the derivatives along a grid line involves only its grid nodes and thus the differentiation matrices stay the same whatever the number of holes inside the domain.

3 EXAMPLES

3.1 Example 1

The PDE and the exact solution are respectively given by

$$\frac{\partial^2 \bar{u}}{\partial x^2} + \frac{\partial^2 \bar{u}}{\partial y^2} = \exp(\sin(x))(\cos(x)^2 - \sin(x)) - \cos(y), \tag{14}$$

$$\bar{u} = \exp(\sin(x)) + \cos(y). \tag{15}$$

The domain of interest is the square $0 \leq x, y \leq 2\pi$ with 9 holes of radius 0.4 (Figure 4).

This problem is solved with different uniform grids, $N_x \times N_y = (21 \times 21, 31 \times 31, \ldots, 91 \times 91)$, and different values of k (different levels of the global regularity). The obtained results are shown in Figure 5. The solution in the physical domain converges as $O(h^{2.4})$, $O(h^{3.9})$, $O(h^{6.0})$, $O(h^{8.1})$ and $O(h^{7.9})$ for the C^0-, C^1-, C^2-, C^3- and C^4-continuity impositions, respectively. For a given grid size, an increase in k results in a better accuracy of the solution.

We also study the effect of the order K of the PDE in the extension domain. The obtained results are shown in Figures 6. With a decrease in K, one has a less accurate solution (Figure 6) but better condition number of matrix $\mathcal{H}^K$. Nevertheless, the fifth-order accuracy is still achieved for $K = 4$.

3.2 Example 2

Consider the following PDE

$$\frac{\partial^2 \bar{u}}{\partial x^2} + \frac{\partial^2 \bar{u}}{\partial y^2} = \sin(x)\sin(y), \tag{16}$$

defined in the square $0 \leq x, y \leq 2\pi$ with 9 holes of radius 0.4 (Figure 4), and subjected to the boundary condition $\bar{u} = 0$. For this problem, the analytical solution is not available. Our results are compared with the one produced by the finite element method (FEM). It can be seen from Figure 7 that the two methods yield similar results. Unlike the FE case, the IRBF solution is defined everywhere in the square.

4 CONCLUSIONS

We have presented a new high-order discretization scheme, based on immersed boundary smooth extension and integrated RBFs, for solving the elliptic equation in a multiply connected domain. The discretization is based on a Cartesian grid, which does not conform to the geometry of the holes; the resultant algebraic systems have only 5 nonzero entries per row. High-order accuracy is achieved by including nodal derivative values in local IRBF approximations, and forcing the solution to be globally smooth in the entire encompassing domain. In solving for the smooth extension of the solution, the constants arising from the process of integrating the RBFs are utilised to include the boundary values of the derivatives in the IRBF approximations, which enables high-order PDE in the extension domain to be enforced at every interior node. Numerical experiments demonstrate that for a high level of the global regularity, high-order accuracy (≥ 4) is still achieved by simply considering the fourth-order PDE in the extension domain.

REFERENCES

[1] Stein, D.B., Guy R.D. and Thomases, B. Immersed boundary smooth extension: A high-order method for solving PDE on arbitrary smooth domains using Fourier spectral methods. *Journal of Computational Physics* (2016) **304**:252–274.

[2] Qadeer, S. and Griffith, B.E. The smooth forcing extension method: A high-order technique for solving elliptic equations on complex domains. *Journal of Computational Physics* (2021) **439**:110390.

[3] Mai-Duy, N. and Strunin D. New approximations for one-dimensional 3-point and two-dimensional 5-point compact integrated RBF stencils. *Engineering Analysis with Boundary Elements* (2021) **125**:12-22.

[4] Mai-Duy, N., Strunin, D. and Karunasena, W. Computing high-order derivatives in compact integrated-RBF stencils. *Engineering Analysis with Boundary Elements* (2022) **135**:369-381.

[5] Mai-Duy, N., Strunin, D. and Karunasena, W. A new high-order nine-point stencil, based on integrated-RBF approximations, for the first biharmonic equation. *Engineering Analysis with Boundary Elements* (2022) **143**:687-699.

[6] Mai-Duy, N., Tien, C.M.T., Strunin, D. and Karunasena, W. An effective high-order five-point stencil, based on integrated-RBF approximations, for the first biharmonic equation and its applications in fluid dynamics. *International Journal of Numerical Methods for Heat & Fluid Flow* (2023) **33**(7):2593-2616.

[7] N. Mai-Duy, Y.T. Gu, A high-order embedded-boundary method based on smooth extension and RBFs for solving elliptic equations in multiply connected domains. *Engineering Analysis with Boundary Elements* (2023) **154**:223-237.

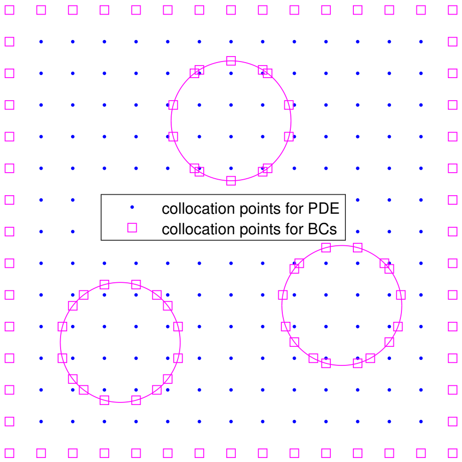

Figure 1: A multiply connected domain: embedded boundaries, Cartesian grid and collocation points. The problem is solved in the domain without holes. Collocation points for enforcing the PDE are all grid nodes inside the outer boundary (blues points), while collocation points for imposing the boundary conditions are points where the grid lines cross the outer and inner boundaries (magenta squares).

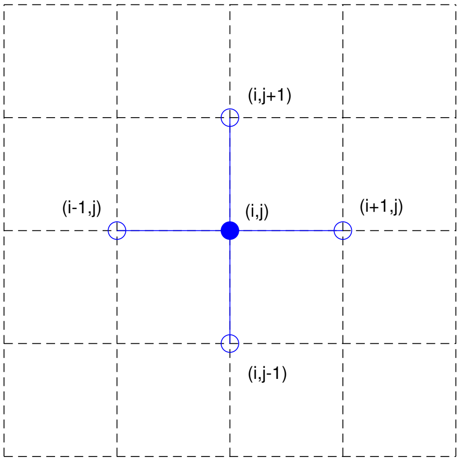

Figure 2: A five-point stencil.

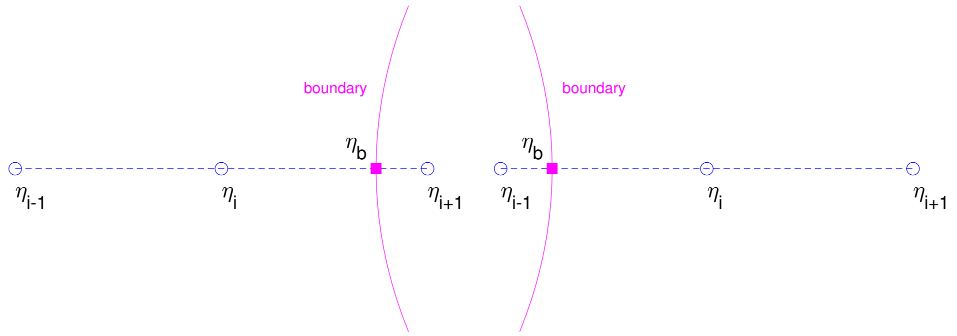

Figure 3: Two possible configurations for a stencil near the immersed boundary ($(\eta_{i-1}, \eta_i, \eta_{i+1})$: grid nodes and η_b: boundary node). They share a common feature: there are two grid nodes in the physical domain and one grid node in the extension domain.

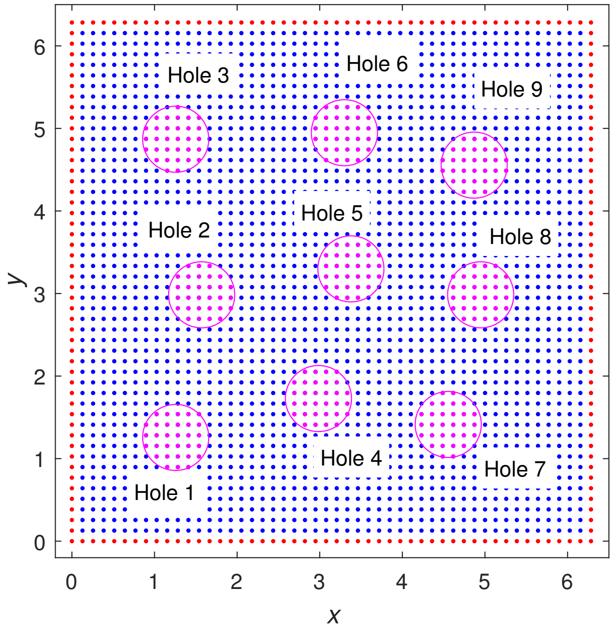

Figure 4: 2D problems, $0 \leq x, y \leq 2\pi$: a domain with 9 holes of radius 0.4

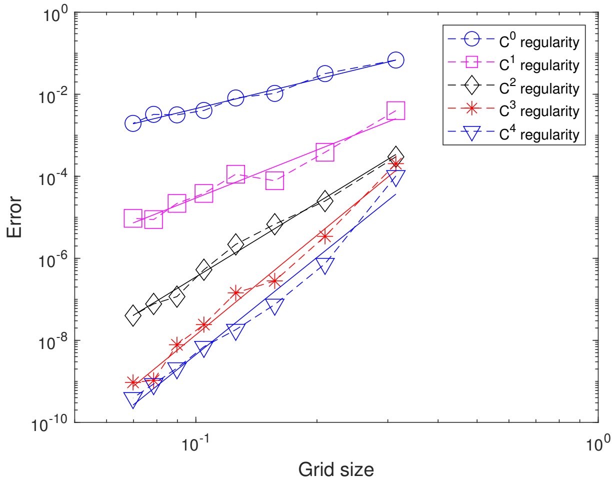

Figure 5: Example 1, $0 \leq x, y \leq 2\pi$, 9 holes of radius 0.4, $(21 \times 21, 31 \times 31, \ldots, 91 \times 91)$: the solution in the physical domain converges as $O(h^{2.4})$, $O(h^{3.9})$, $O(h^{6.0})$, $O(h^{8.1})$ and $O(h^{7.9})$ for the C^0-, C^1-, C^2-, C^3- and C^4-continuity impositions, respectively.

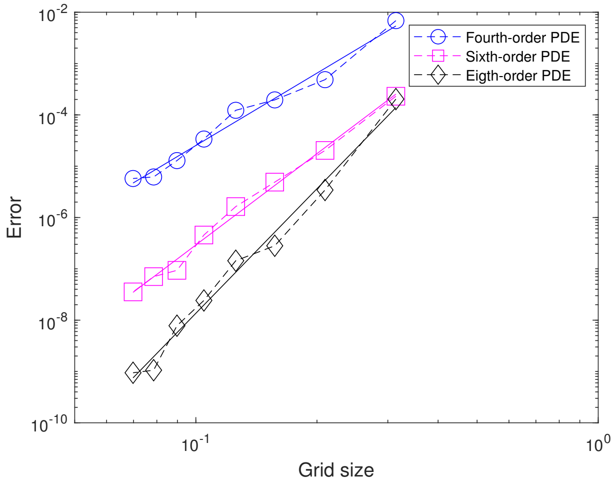

Figure 6: Example 1, $0 \leq x, y \leq 2\pi$, 9 holes of radius 0.4, global C^3 regularity, $(21 \times 21, 31 \times 31, \ldots, 91 \times 91)$: the solution in the physical domain converges as $O(h^{4.7})$, $O(h^{5.9})$, and $O(h^{8.1})$ when the order of the PDE in the extension domain is chosen as 4, 6 and 8, respectively.

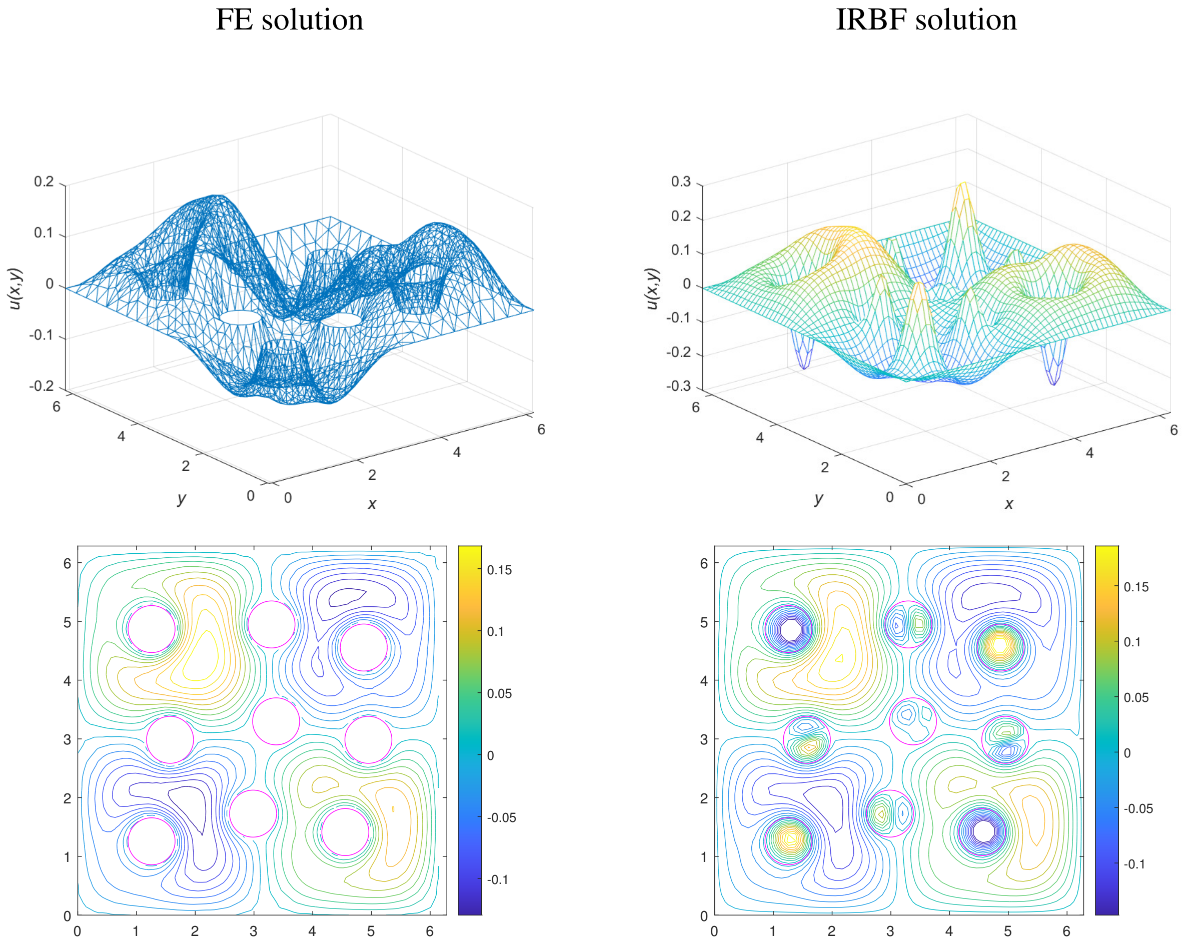
FE solution

IRBF solution

Figure 7: Example 2, $0 \leq x, y \leq 2\pi$, 9 holes of radius 0.4, global C^4 regularity, fourth-order PDE in the extension domain: FE and IRBF solutions. The solution is smooth in the entire computational domain for the latter but not defined in the holes for the former.